

Effect of a Potential Jump in a Magnetic Junction upon Spin Injection by an Electric Current on the Effectiveness of Electromagnetic Wave Radiation

E. A. Vilkov^a and S. G. Chigarev^{a, *}

^a*Kotelnikov Institute of Radio Engineering and Electronics, Russian Academy of Sciences, Fryazino, 141190 Russia*

**e-mail: chig50@mail.ru*

Received July 29, 2019; revised August 30, 2019; accepted September 27, 2019

Abstract—Results are presented from studying the effect a jump in potential has on the modes of operation of different magnetic junctions, including the Ni/NiO/Fe tunnel magnetic junction. The difference between the effectiveness of radiation in them is explained by the effect of jumps in potential have on the formation of Fermi quasi-levels in spin-energy sub-bands.

DOI: 10.3103/S106287382001027X

INTRODUCTION

Magnetic nanostructures are of great interest today because they offer potential benefits in many areas. One possibility is creating sources of electromagnetic waves, including the least exploited range of terahertz frequencies [1–3]. The advantages of using sources of THz signals in outer space to determine locations and for communication between satellites should especially be noted. The general principle of operation for devices based on magnetic heterostructures with current flowing through them relies on spin polarization of the flow of free electrons in one of their magnetic layers (called injector) and interaction between the spin-polarized current and the magnetization of the crystal lattice of the other layer (the operating one). Depending on different conditions (especially the current density), either we can modify the magnetization of a localized region of the operating layer's crystal lattice or the spin state of the electron flow can be altered by some electrons moving from one energy sub-band to another, accompanied by the spin reorientation (the spin–flip process). The latter effect is used in spin-injector sources of THz signals.

It is known that interface resistance occurs in magnetic heterostructures in the area of contact between layers [4]; its value is determined by the orientation of spins of free electrons relative to the magnetization of the operating layer. Resistance is weaker for spins parallel to the direction of magnetization (major electrons) than for spins with antiparallel orientation (minor spins). The difference in resistance results in a situation when electrons traveling through the interface acquire different energies from the power source. The difference between the energies of the electrons distributed among the spin sub-bands is described by

the exchange splitting of the spin sub-bands with the formation of Fermi quasi-levels in each of the sub-bands [5]. This splitting determines the energy emitted by an electron upon a spin-flip transition. The magnitude of exchange splitting also determines the efficiency of the generator, since the power of the signal generated by a spin-injector source is proportional to the total energy of the emitted quanta.

Despite the obvious effect the magnetic interface has on the formation of Fermi quasi-levels (and thus the efficiency of the spin-injector source), this problem has not been considered separately. In this work, we present the first results on the effect the interfaces in two magnetic junctions have on the efficiency of spin-injector generators, obtained by comparing their operating characteristics. The studied magnetic junctions were made of identical ferromagnetic layers. In one, however, they were in direct contact, while a tunnel magnetic barrier was used in the other, and the layers were separated by a thin nonmagnetic insulating spacer [6, 7]. Antiferromagnetic semiconductor NiO was used as the spacer because it does not totally destroy the exchange interaction between the magnetic layers, due to the effect of sublattice skew in the antiferromagnetic caused by a spin-polarized current [8]. This allowed us to explain the difference between the efficiency of the investigated spin-injector sources mainly from the difference between the interfaces in our magnetic junctions.

PHYSICAL MODEL OF THE PROCESS

Conduction electrons in our model were distributed over spin sub-bands and had an isotropic parabolic energy spectrum with a certain effective mass.

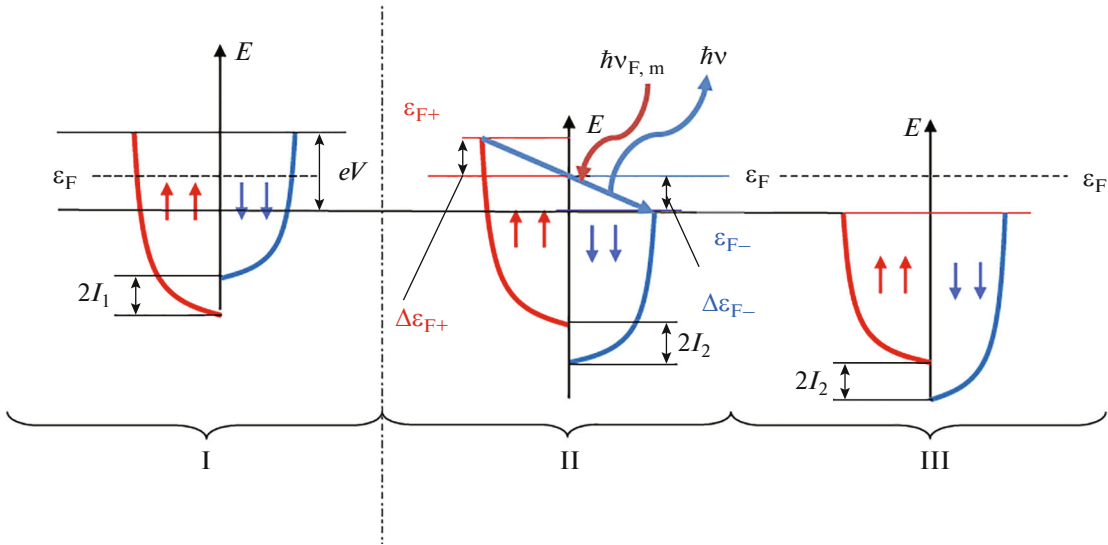


Fig. 1. Scheme of the energy of electron sub-bands and Fermi quasi-levels: I, in the first ferromagnetic layer; II, for nonequilibrium electrons in the second ferromagnetic layer; III, for equilibrium electrons in the second ferromagnetic layer outside the injection region. Label $\hbar v_m$ shows the absorption of a photon's magnon; $\hbar v$ denotes THz radiation.

Figure 1 shows the scheme of a typical magnetic junction used in spin-injector terahertz sources. An ultrathin buffer layer of a dielectric material or nonmagnetic metal can be inserted in the magnetic junction between ferromagnetic layers I and II. According to [6, 7], this eliminates exchange interaction between the magnetic layers and ensures conditions in which the electrons that are minor in the operating layer can populate energy levels above the equilibrium Fermi level. The transformation of energy in the sub-bands as the current flows from the injector to the operating layer (from region I to region II) is shown in Fig. 1 [5]. Spins not compensated for are injected into operating layer II, and Fermi quasi-levels for the average populations of the spin sub-bands form. After the spins not compensated for relax, the electrons exit through region III, which acts as a collector.

We must consider the current flowing through the magnetic junction interface to understand the process of energy transfer from the power source to the spin-injector radiation. According to [4], the current passing through the magnetic junction can be represented as flows of conduction electrons with different spin orientations that encounter the different resistance of the interface. This allows us to present the total energy carried by the flow in the spin injection as [9]

$$W = W_{\uparrow} + W_{\downarrow} = \frac{1}{2e} j(\zeta_{\uparrow} + \zeta_{\downarrow} + 2e\varphi) + \frac{1}{2\mu_B} J_{zx}(\zeta_{\uparrow} - \zeta_{\downarrow}) \cos \chi, \quad (1)$$

where e is the electron charge; j is the total current density; J_{zx} is the spin flow of the electrons; $\zeta_{\uparrow\downarrow}$ denotes the chemical potentials (Fermi quasi-levels in

the sub-bands [9]); φ is the electrostatic potential; μ_B is the Bohr magneton; χ is the angle between the magnetizations of the neighbor layers; and $W_{\uparrow\downarrow}$ represents partial energy flows of the electrons with different spin orientations (\uparrow for those oriented along the magnetization and \downarrow for antiparallel spins). Allowing for the continuity of the energy flow at the $-0|+0$ interface, we obtain two conditions from Eq. (1) according to [9]:

$$(\zeta_{1\uparrow} - \zeta_{1\downarrow})_{x=0} = (\zeta_{2\uparrow} - \zeta_{2\downarrow})_{x=+0} \cos \chi, \quad (2a)$$

$$(\zeta_{1\uparrow} + \zeta_{1\downarrow})_{x=0} - (\zeta_{2\uparrow} + \zeta_{2\downarrow})_{x=+0} = 2e[\varphi(+0) - \varphi(-0)]. \quad (2b)$$

Correlation (2) describes processes of a magnetic nature, while (3) corresponds to electrostatic processes. It follows from Eq. (3) that a potential difference will arise at the junction of magnetic layers even when there is no intermediate layer. The power source thus ensures drop in voltage ΔV across the magnetic junction interface when current flows through the magnetic junction. The drop is determined for optimum angle $\chi = \pi$ by the formula

$$\Delta V = V - V_0 = jZ_1Z_2 \frac{(-Q_1 - Q_2)^2}{Z_1 + Z_2} = j \frac{Z_1Z_2}{Z_1 + Z_2} (Q_1 + Q_2)^2. \quad (3)$$

Here, V is the voltage of the power source; $V_0 = \left(\frac{L_2 + L_1}{\sigma_2 + \sigma_1} \right) + \frac{1}{e}(\bar{\zeta}_1 - \bar{\zeta}_2)$ is the voltage at the magnetic junction in the state of spin equilibrium (the first term is the drop in voltage across the active resistance

of the layers, while the second term corresponds to the contact potential difference); $\bar{\zeta}_{12}$ is the chemical potential in the state of spin equilibrium;

$Z_{12} = \frac{\bar{I}_{12}}{\sigma_{12}} (1 - Q_{12}^2)^{-1}$ is the spin resistance of the layers;

$Q_{12} = \frac{\sigma_{12}^{\uparrow} - \sigma_{12}^{\downarrow}}{\sigma_{12}^{\uparrow} + \sigma_{12}^{\downarrow}}$ is the polarization of conductivity

of either layer 1 or 2; $\sigma_{12}^{\uparrow\downarrow} = \mu_{12}^{\uparrow\downarrow} \times n_{12}^{\uparrow\downarrow}$ is the partial conductivity determined by electron mobility $\mu_{12}^{\uparrow\downarrow}$ with either spin in a given layer; and $n_{12}^{\uparrow\downarrow}$ is the partial concentration of electrons in the layers. Note that ΔV in (4) is considered for the total (summed) resistances of the layers.

As an example, let us consider the emergence of a jump in potential at the interface during a flow of electrons with different spin orientations for optimum angle value $\chi = \pi$. Note that the major electrons in the injector become minor ones in the operating region, since they enter the environment with the opposite direction of magnetization because the spin state remains unchanged. An analogous situation is observed for the minor electrons in the injector. The spin states of the electrons in the sub-bands remaining intact upon moving from the injector to the operating region are designated as (+) for the major electrons in the injector and (−) for the minor electrons. As noted above, the spin resistances for the flows are different; they also differ for one and the same flow in different layers. According to [4], $Z_{1\uparrow}^+ < Z_{2\uparrow}^+$, $Z_{1\downarrow}^- > Z_{2\downarrow}^-$. Allowing for this, expression (3) can be rewritten as

$$\begin{aligned} & (\zeta_{1\uparrow}^+ - \zeta_{2\uparrow}^+ + e(\varphi_2^+ - \varphi_1^+)) \\ & + (\zeta_{1\downarrow}^- - \zeta_{2\downarrow}^- + e(\varphi_2^- - \varphi_1^-)) = 0. \end{aligned} \quad (4)$$

Let us consider a small region without relaxation (without spin-flip transitions), so the current densities of the spin flows in the injector and operating region remain constant. This allows us to relate potentials φ_{12}^{\pm} with the magnetoresistances of the layers $Z_{12\uparrow\downarrow}^{\pm}$: $\varphi_1^+ = j^+ Z_{1\uparrow}^+$, $\varphi_2^+ = j^+ Z_{2\uparrow}^+$, $\varphi_1^- = j^- Z_{1\downarrow}^-$, $\varphi_2^- = j^- Z_{2\downarrow}^-$.

Consequently, $\varphi_2^+ > \varphi_1^+$, $\varphi_2^- < \varphi_1^-$, which leads to

$$\Delta\varphi^+ = \varphi_2^+ - \varphi_1^+ > 0, \quad (5)$$

$$\Delta\varphi^- = \varphi_2^- - \varphi_1^- < 0. \quad (6)$$

Relation (5) shows that electrons that are major in the injector acquire energies higher than the equilibrium value (the equilibrium Fermi level) as they travel through the interface. At the same time, Eq. (6) shows that the minor electrons from the injector acquire energies lower than the equilibrium value. In Fig. 1, this process is depicted as the emergence of Fermi quasi-levels in the sub-bands of region II.

The difference between potentials at the insulating layer in a tunnel magnetic junction is determined by the height of the energy barrier. The difference in potential at the magnetic junction interface can be modified by choosing the correct insulating layer.

Two magnetic junctions made from Fe and Ni ferromagnetic layers were used to study the effect the difference between interface potentials has on the generation of electromagnetic waves upon spin injection in the magnetic junction. A structure of the rod–film type was used in one of them [10]; a steel rod with a sharp tip less than 50 μm in diameter was in direct contact with a nickel film 30 nm thick. A tunnel magnetic junction formed by crossing strips of Fe and Ni 30 nm thick and 50 μm wide was used in the second structure. The layers in the crossing area were separated by a spacer made from antiferromagnetic semiconductor NiO 5 nm thick. Estimates show that the potential barrier for the minor electrons, associated with the exchange *sd*-interaction at the Ni–Fe interface, was about 0.1 eV. At the same time, a layer of NiO several nanometers thick is known to provide a potential barrier of around 0.2 eV and thus ensures the necessary difference of potentials between the ferromagnetic layers for the tunneling of nonequilibrium spins into the operating region.

EXPERIMENTAL

Experimental studies were performed to make comparative estimates of how the interfaces in the junctions influence the efficiency of spin-injector generators. As in [11], the efficiency of a given source was defined by that of its power, and by the initial current. In addition to these parameters, volt–ampere characteristics were compared. Our experiments thus included measuring the radiation power, voltage at the source, and the corresponding current. The values obtained from our measurements were used to build the corresponding dependences.

A GSS 3–123 harmonic voltage generator was used as the power source in our experimental setup; it applied harmonic voltage with amplitudes of up to 10 V and a frequency of 6 Hz onto the spin-injector source. This provided the optimum terahertz signal frequency of 12 Hz for the operation of the registering detector. A Tydex GC-1P optoacoustic converter (Golay cell) was used as the detector. High-pass filter blocking signals with frequencies below 1.25 THz were also used. The values of interest were acquired using an Aktakom 3117 analog-to-digital converter and registered on a PC. The alternating voltage applied to the source and the current passing through it were recorded simultaneously. The resistance of the source at a given voltage was determined from the obtained volt–ampere characteristics.

In both cases, measurements were made without a focusing lens, and the distance between the source and

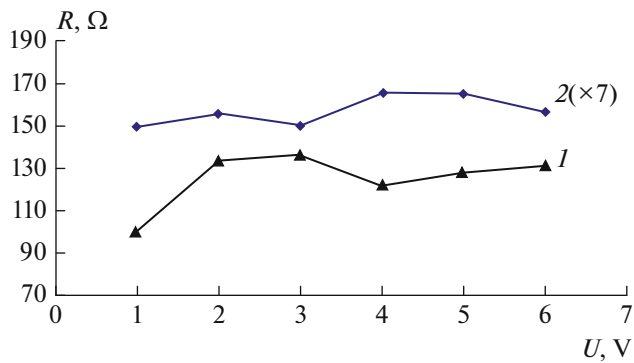


Fig. 2. Dependence of resistance R of the source on the applied voltage: curve 1 for the structure with a tunnel junction; curve 2 (amplified 7 times) for the rod–film structure.

the Golay cell was 50 mm. Radiation power in the control unit of the Golay cell was measured in millivolts. The values in millivolts were converted to microwatts according to the cell's calibration curve and allowing for attenuation in the circuits and in the substrate.

RESULTS AND DISCUSSION

The behavior of the resistance of the radiation sources with the tunnel junction (curve 1) and the rod–film structure (curve 2) upon varying the voltage at the sources is shown in Fig. 2.

Note that the range of operating voltages was nearly the same for both sources, and the initial voltage at which the radiation was detected in both cases ~ 2 V. The emergence of radiation altered the dependence of the resistance on the voltage. The growth of the resistance slowed for the source with the tunnel junction, while a drop in resistance was observed for the rod–film structure. As expected, the resistance of the tunnel junction was considerably higher than that of the direct contact of the ferromagnetic elements (by nearly 5–6 times). Let us now consider the effect the spacer had on the efficiency of the source.

The effect the spacers in the two types of magnetic junctions had on their power is shown in Fig. 3 as the dependence of the radiation power on the current. The data show that the spin-injector source with the NiO spacer had remarkably higher efficiency than the generator without the spacer. The initial current in the source with the tunnel junction is nearly 5–6 times lower than in the one with the magnetic junction in which magnetic layers in direct contact were used. In addition, a much weaker current is needed at a given voltage to achieve the same radiation power; i.e., the efficiency of the source with the tunnel junction is higher.

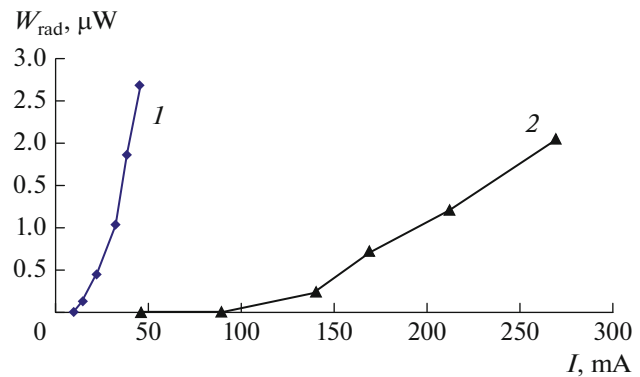


Fig. 3. Dependence of radiation power W_{rad} on current I . Curve 1 shows the radiation power when using the tunnel magnetic junction; curve 2, the radiation power of the rod–film structure.

Numerical estimates can help us compare the efficiency of the given radiation sources. We estimate the power consumed by the sources and providing equal signal powers of $2 \mu\text{W}$. For the tunnel magnetic junction, we obtain $U = 5.6$ V, $I = 45$ mA, and $W = 0.25$ W; for the rod–film structure, $U = 6$ V, $I = 270$ mA, and $W = 1.6$ W. The efficiency of the source with the tunnel junction is thus nearly 6 times higher than that of the one with the direct contact between layers. The initial currents in the investigated generators also differ by nearly 6 times. On the whole, the efficiency of the generator with the tunnel junction is about 6 times greater than that of the source based on the rod–film structure. Note too that the resistances of the studied sources also differ sixfold. Assuming that the drop in interface voltage in the magnetic junction was proportional to its resistance, we obtain a direct correlation with the generator's efficiency.

The efficiency of a spin-injector source is generally related to the jump in potential that arises at the interface between magnetic layers and pulls minor electrons from the operating region to high-energy levels above the equilibrium Fermi level. As the difference between potentials increases, the population of the spin sub-bands above the equilibrium Fermi level also grows, and the number of quantum transitions occurring per unit of time increase, along with the energy of the emitted quanta.

CONCLUSIONS

Our results demonstrate the effect the difference between the potentials that arise at an interface between magnetic layers has on the efficiency of a spin-injector generator of radiation. Energy levels above the equilibrium Fermi level, occupied by electrons with nonequilibrium spins, are determined by this difference between potentials. The greater this drop in voltage, the higher the efficiency of the radiation source.

ACKNOWLEDGMENTS

The authors thank V.I. Malikov and A.V. Chernykh for their assistance in performing this study.

REFERENCES

1. Krivorotov, N., Emley, N.C., Sankey, J.C., et al., *Science*, 2005, vol. 307, p. 228.
2. Kadigrobov, A., Ivanov, Z., Claeson, T., et al., *Europhys. Lett.*, 2004, vol. 67, p. 948.
3. Gulyaev, Yu.V., Zilberman, P.E., Malikov, I.V., Mikhailov, G.M., Panas, A.I., Chigarev, S.G., and Epshtein, E.M., *JETP Lett.*, 2011, vol. 93, no. 5, p. 259.
4. Valet, T. and Fert, A., *Phys. Rev. B*, 1993, vol. 48, no. 10, p. 7099.
5. Vilkov, E.A., Mikhailov, G.M., Chigarev, S.G., Gulyaev, Yu.V., Korenivskii, V.N., Nikitov, S.A., and Slavin, A.N., *J. Commun. Technol. Electron.*, 2016, vol. 61, no. 9, p. 995.
6. Fert, A., George, J.-M., Jaffres, H., et al., *Europhys. News*, 2003, vol. 34, no. 6, p. 227.
7. Berger, L., *Phys. Rev. B*, 1996, vol. 54, p. 9353.
8. Gulyaev, Yu.V., Zil'berman, P.E., Kasatkin, S.I., Mikhailov, G.M., and Chigarev, S.G., *J. Commun. Technol. Electron.*, 2013, vol. 58, no. 7, p. 716.
9. Gulyaev, Yu.V., Zil'berman, P.E., and Chigarev, S.G., *J. Commun. Technol. Electron.*, 2015, vol. 60, no. 5, p. 411.
10. Gulyaev, Yu.V., Zil'berman, P.E., Epshtein, E.M., et al., RF Patent 2464683, 2012.
11. Gulyaev, Yu.V., Vilkov, E.A., Chigarev, S.G., Kulikov, R.S., Safin, A.R., Udalov, N.N., Davydenko, R.S., Kolesnikov, A.G., Ognev, A.V., Mikhailov, G.M., Chernykh, A.V., and Il'in, S.V., *J. Commun. Technol. Electron.*, 2018, vol. 63, no. 8, p. 928.

Translated by S. Efimov